International Journal of Scientific Research in Physics and Applied Sciences
Vol.**12**, Issue.**2**, pp.**55-65**, April **2024**
E-ISSN: 2348-3423
Available online at: www.isroset.org

Research Article

Application of the Caputo-Fabrizio Fractional Model for Investigating MHD Blood Flow in Permeable Bifurcated Arteries Subjected to an Inclined Magnetic Field: Relevance to Tumor Therapy

Isah Abdullahi[1*], Ali Musa[2]

[1]Dept. of Mathematical Sciences, Abubakar Tafawa Balewa University, Bauchi, Nigeria
[2]Dept. of Mathematics, Yobe State, University, Damaturu, Nigeria

**Corresponding Author: isahabdullahi7474@gmail.com, Tel: +2347039747474*

Received: 18/Feb/2024; **Accepted**: 20/Mar/2024; **Published**: 30/Apr/2024

Abstract— This article introduces a model employing fractional-order time derivatives to describe magneto-hydrodynamic blood flow in bifurcated arteries subjected to an inclined magnetic field. It also considers thermal radiation, heat source effects, and chemical reactions relevant to tumor treatments. The Caputo-Fabrizio fractional derivative framework is utilized, and the problem is tackled using Laplace transform and the method of indeterminate coefficients. Analytical expressions for blood flow velocity, temperature, and concentration are derived. Graphical simulations are performed to investigate the impacts of various parameters, such as the order of Caputo-Fabrizio fractional derivative, magnetic field strength, thermal radiation, chemical reaction rate, heat source intensity, and Schmidt number. The results highlight the significant influence of the fractional order parameter on blood velocity, temperature, and concentration, particularly in shorter time frames. Moreover, parameters like inclined magnetic field, heat source, and chemical reaction rates are shown to exert considerable control over arterial wall blood velocity, temperature, and concentration. These findings have important implications for biomedical engineering and pathology applications.

Keywords— Caputo-Fabrizio, Bifurcated Arteries, Inclined Magnetic Field, Tumor Treatment

1. Introduction

The investigation of bio-fluid motion, especially blood flow affected by magnetic fields, is attracting attention in fluid mechanics, within the realm of bio-magnetic fluid dynamics (BFD). This area holds significant importance in medical sciences, including applications such as drug delivery using magnetic particles, homeostasis, and cancer tumor treatment. Blood, considered a bio-magnetic fluid, displays magnetic properties due to its haemoglobin molecules [1,2,3]. For example, [4] studied magneto-hydrodynamic flow and heat transfer in an overlapping constricted artery under periodic body acceleration and temperature-dependent viscosity. Several studies [5,6,7,8,9,10] have characterized blood as a non-Newtonian fluid, demonstrating magneto-hydrodynamic (MHD) characteristics due to its electrical conductivity. [11] investigated MHD flow and heat transfer in a narrowed artery, while [12] analyzed ferromagnetic blood flow through a narrowed artery with a permeable wall. The concept of fractional-order derivatives, initially introduced by Leibniz in 1832, has found applications in various research areas, particularly in understanding the rheological properties and complex dynamics of diverse fluids [13,14,15,16,17,18,19]. Blood's behavior varies; it may adhere to Newtonian fluid dynamics in large arteries under high shear rates, but even in such scenarios, it exhibits non-Newtonian behavior, as noted by [20].

At low shear rates, blood demonstrates behavior similar to that of a Casson fluid [21], as affirmed by multiple researchers [22,23,24]. [25] proposed a fractional-order model for Casson fluid blood flow, employing Hankel transform and Laplace transform techniques for precise solutions, while [26] developed a mathematical model for MHD blood flow in a tube containing dusty magnetite particles, utilizing the fractional Caputo time derivative. [27,28] respectively examined oxygen diffusion dynamics at the tissue capillary level and the intricacies of blood vessel responses under various forces using Caputo-Liouville and Caputo-Fabrizio fractional-order models. However, to the best of our knowledge, no prior efforts have been made to investigate a fractional-order time-derivative model of magnetohydrodynamic (MHD) blood flow through permeable bifurcated arteries with an inclined magnetic field, incorporating heat and mass transfer phenomena alongside thermal radiation. The study of blood flow through porous

media holds significance in biofluid dynamics. Examples include the capillary endothelium surrounded by alveoli and the presence of fatty plaques within arterial lumen segments, both considered porous media. The permeability of a porous medium, indicating flow conductivity, is a defining characteristic. Various researchers have explored the movement of physiological fluids through porous media under diverse conditions. [29,30] developed models for blood flow through porous media using the Brinkman equation, while [31] applied Darcy's law to depict blood as the liquid in the porous medium. Additionally, [32] introduced a mathematical model to investigate blood flow, heat, and mass transfer within a porous medium channel, utilizing the combined Darcy-Brinkman-Forchheimer model.

2. Related Work

In hyperthermia therapy, the transfer of radiant heat within blood vessels is critically significant, especially in oncology. Several studies have computationally evaluated the influence of magnetic fields and thermal radiation on arterial blood flow. Additionally, investigations have explored electromagnetohydrodynamic effects and the combined impacts of external radiation and magnetic fields on blood flow in large vessels. Furthermore, research has delved into heat transfer processes in second-class MHD fluids and the peristaltic motion of blood containing particle-liquid suspensions with variable viscosity [33,34,35]. The vibrational environment profoundly affects blood flow, with body acceleration leading to various health concerns. Mathematical models addressing oscillating blood flow under body acceleration have been examined, alongside hydro elastic single wave propagation in uniform flow channels [36,37]. Moreover, studies have investigated pulsatile blood flow through narrowed arteries under the joint influence of an external magnetic field and periodic body acceleration. MHD flow holds significant importance in medical applications, particularly in tumor treatment and the mitigation of bleeding from injuries [38,39,40]. Analytical solutions have been derived for non-Newtonian MHD nanofluids with temperature-dependent viscosity, as well as for peristaltic flow and heat transfer of nanofluids. Models incorporating fractional blood flow in oscillatory arteries along with thermal radiation have also been developed. Investigations have explored the effects of Caputo's time-fractionated derivatives and external magnetic fields on blood flow parameters in cylindrical domains [41,42].

In this investigation, we employ a Newtonian fluid approach to characterize the fractional-order time derivative governing magnetohydrodynamic (MHD) blood flow through bifurcated arteries in the presence of an inclined magnetic field, while simultaneously considering the coupled influences of heat transfer and blood flow concentration. Building upon existing literature, we develop a comprehensive time-sharing model with the aim of understanding the impact of heat and mass transfer on MHD blood flow through bifurcated arteries under an inclined magnetic field, particularly in the context of tumor treatment. Additionally, the blood flow encounters exposure to a magnetic field. We utilize the indeterminate coefficient method and Laplace transform techniques to derive the exact solution. The study's findings are succinctly illustrated through various graphical representations, delineating the effects of the different parameters under consideration.
Top of Form

3. Methodology

From a numerical perspective, the following assumptions are made: Blood is characterized as a Newtonian, compressible, homogeneous fluid with adhesive properties, flowing through a non-directing, equal plate channel from the trunk to the branches. The mass flow rate at any cross-sectional area perpendicular to the flow direction is given by m=2bv, where v represents the mean velocity of the flow, b denotes the width of the channel, and ρ signifies the density of blood. The bifurcating partition does not affect the velocity of the mass flow at any cross-section of the expanded channel, which remains equal to m/2 (refer to Fig 1). Due to the low magnetic Reynolds number considered, the magnetic field is applied at an angle to the flow direction. Consequently, it is assumed that the induced magnetic field and electric field generated by the blood flow are negligible. Since the bifurcation angle is zero, the blood flow region is divided into two streams that run parallel to the major artery.

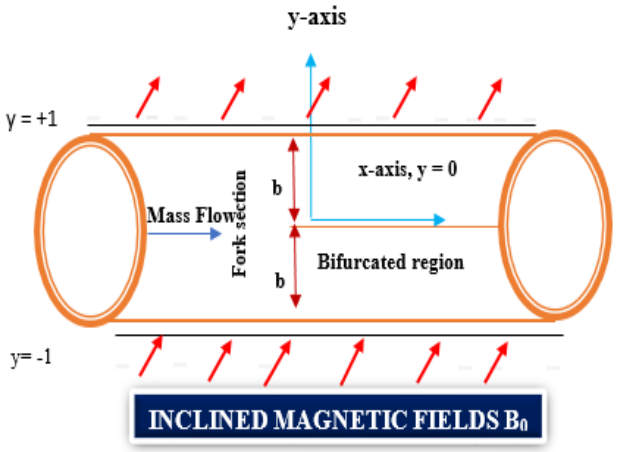

Fig.1. Physical Flow Geometry

Basic flow Equations and solutions
Blood flows through a permeable medium as two boundary layers under the influence of a magnetic field, with heat transfer occurring in accordance with the assumptions outlined in the numerical formulation. Let u and v represent the velocity components in the x and y directions of the flow field at time t, and δ denotes the thickness and viscosity of the blood, while p represents the blood pressure. Additionally, KT denotes thermal conductivity, Cp signifies the specific heat capacity at constant pressure, Q represents the amount of heat, T signifies the temperature, β represents the volumetric expansion coefficient, θ represents temperature distribution, θ signifies the angle of inclination of the applied magnetic field, and K represents the porosity parameter.

$$\left.\begin{aligned}\frac{\partial \bar{u}}{\partial \bar{t}}+\frac{1}{\rho}\frac{\partial \bar{p}}{\partial \bar{x}}=\frac{\eta}{\rho}\frac{\partial^2 \bar{u}}{\partial \bar{y}^2}+g\beta(T-T_\infty)^{-}\\ +g\beta'(C-C_\infty)^{-}-\frac{\sigma B_0^2\sin^2\phi}{\rho}\bar{u}-\frac{\bar{u}}{\bar{k}}\end{aligned}\right\} \quad (1)$$

$$\left.\frac{\partial \bar{T}}{\partial \bar{t}}=\frac{k_T}{\rho C_\rho}\frac{\partial^2 \bar{T}}{\partial \bar{y}^2}+\frac{Q}{\rho C_\rho}(T-T_\infty)^{-}-\frac{\partial \bar{q}}{\partial \bar{y}}\right\} \quad (2)$$

$$\left.\frac{\partial \bar{u}}{\partial \bar{x}}+\frac{\partial \bar{v}}{\partial \bar{y}}=0\right\} \quad (3)$$

where,

$\frac{\partial}{\partial t}$ is the material time derivative. However, for the delivery of drugs (concentration) in magnetohydrodynamic blood flow through permeable bifurcated arteries, the concentration equation in dimensionless form is provided as follows:

$$\frac{\partial \bar{C}}{\partial \bar{t}}=D\frac{\partial^2 \bar{C}}{\partial \bar{y}^2}+G \quad (4)$$

where

$G=-k_1(C-C_\infty)^{-}$ is any constant (G = 1) and D is the diffusion coefficient.

$$\left.\begin{aligned}\theta=\ell^{-\lambda^2 t},u=\ell^{-\lambda^2 t},v=\ell^{-\lambda^2 t},C=\ell^{-\lambda^2 t},\ y=-1\\ \theta\to 0,\ u\to 0,\ v\to 0,\ C\to 0\ at,\qquad y=1\end{aligned}\right\} \quad (5)$$

The governing equations (1) to (4) can be converted into dimensionless form by employing suitable normalization parameters. Thus, we introduce non-dimensional parameters to simplify our study, which are:

$$\left.\begin{aligned}x=\frac{\bar{x}}{b},\ y=\frac{\bar{y}}{b},\ u=\frac{\bar{u}}{mu_{HS}/2b\rho},\\ v=\frac{\bar{v}}{mu_{HS}/2b\rho},h(x,t)=\frac{d\bar{p}/d\bar{x}}{u_{HS}\eta m/2b^3\rho}\\ k=\frac{\bar{k}}{\left(b^2\rho/\eta\right)}\quad,C=\frac{\bar{C}(2b^3\rho^2)}{m\eta u_{HS}},\bar{q}=-16\delta' T_0^3\Big/3k'\frac{\partial \bar{T}}{\partial \bar{y}}\\ \theta=\frac{\bar{\theta}(2b^3\rho^2)}{m\eta u_{HS}},\tau=\frac{\eta}{\rho},t=\frac{\bar{t}}{\left(b^2\rho/\eta\right)},\end{aligned}\right\} \quad (6)$$

By applying (5) and (6) to equations (1)- (4) and dropping the bars we obtain:

$$\frac{\partial u}{\partial t}+h=\frac{\partial^2 u}{\partial y^2}+g\beta\theta+g\beta' C-M^2\sin^2\phi-\frac{u}{k} \quad (7)$$

$$\frac{\partial \theta}{\partial t}=\left(\frac{1}{\pi p_r}+R\right)\frac{\partial^2 \theta}{\partial y^2}+\left(\frac{S}{\pi p_r}\right)\theta \quad (8)$$

$$\frac{\partial u}{\partial x}+\frac{\partial v}{\partial y}=0 \quad (9)$$

$$\frac{\partial C}{\partial t}=\frac{1}{S_C}\frac{\partial^2 C}{\partial y^2}-\omega C \quad (10)$$

where

$$M^2=\frac{\sigma B_0^2}{\rho}$$

$$p_r=\frac{\rho C_\rho}{k_T},\quad R=\frac{16\delta' T_0^3}{3k'\tau},\quad S=\frac{Qb^2}{k_T},S_C=\frac{\tau}{bD},\omega=\frac{k_1 b^2}{\tau}$$

The magnetic field parameter, Prandtl number, thermal radiation parameter, heat source parameter, Schmidt number, and chemical reaction parameter will be examined accordingly. Consequently, we will address the time fractional momentum equations, utilizing the Caputo-Fabrizio fractional derivative.

$$\left.\begin{aligned}{}^{CF}D_t^\alpha u(y,t)=\frac{1}{1-\alpha}\int_0^t\frac{\partial u(y,\tau)}{\partial \tau}exo\left(-\frac{\alpha(t-\tau)}{1-\alpha}\right)d\tau,\\ 0<\alpha<1\\ L\left\{{}^{CF}D_t^\alpha u(y,t)\right\}=\frac{su(y,s)-u(y,0)}{(1-\alpha)s+\alpha}\end{aligned}\right\} \quad (11)$$

$$u(y,0)=0 \quad (12)$$

Now the fractional differential equation with Caputo-Fabrizio derivative corresponding to equations (7), (8) and (10) are:

$$\left.\begin{aligned}{}^{CF}D_t^\alpha u(y,t)+h=\frac{\partial^2 u}{\partial y^2}+g\beta\theta+g\beta' C-\\ M^2\sin^2\phi-\frac{u}{k}\end{aligned}\right\} \quad (13)$$

$${}^{CF}D_t^\alpha\theta(y,t)=\left(\frac{1}{\pi p_r}+R\right)\frac{\partial^2\theta}{\partial y^2}+\left(\frac{S}{\pi p_r}\right)\theta \quad (14)$$

$${}^{CF}D_t^\alpha C\ (y,t)=\frac{\partial C}{\partial t}=\frac{1}{S_C}\frac{\partial^2 C}{\partial y^2}-\omega C \quad (15)$$

Applying Laplace transform to equations (13) to (15), and using the boundary condition (12):

$$\left.\begin{aligned}\frac{su(y,s)}{(1-\alpha)s+\alpha}+h=\frac{\partial^2 \bar{u}}{\partial \bar{y}^2}+g\beta\bar{\theta}+g\beta'\bar{C}-\\ M^2\sin^2\phi-\frac{\bar{u}}{k}\end{aligned}\right\} \quad (16)$$

$$\frac{su(y,s)}{(1-\alpha)s+\alpha}=\left(\frac{1}{\pi p_r}+R\right)\frac{\partial^2\bar{\theta}}{\partial \bar{y}^2}+\left(\frac{S}{\pi p_r}\right)\bar{\theta} \quad (17)$$

$$\frac{su(y,s)}{(1-\alpha)s+\alpha}=\frac{1}{S_C}\frac{\partial^2 \bar{C}}{\partial \bar{y}^2}-\omega\bar{C} \quad (18)$$

4. Analytical solutions

Let the arbitrary solutions of equations (9), (16), (17) and (18) be,

$$\bar{u} = \bar{F}(y)\frac{1}{s+\lambda^2},, \tag{19}$$

$$\bar{\theta} = \bar{H}(y)\frac{1}{s+\lambda^2}, \tag{20}$$

$$\bar{v} = \bar{G}(y)\frac{1}{s+\lambda^2} \tag{21}$$

$$\bar{C} = \bar{I}(y)\frac{1}{s+\lambda^2} \tag{22}$$

then the boundary conditions in (5) reduce to;

$$\left.\begin{aligned} &H=1,\ I=1,\quad F=1,\quad y=-1\\ &H\to 0, I\to 0, F\to 0,\qquad y=1\end{aligned}\right\} \tag{23}$$

Reduced governing equations of motions with arbitrary solution are:

$$\frac{d^2\bar{F}}{dy^2} - A_2\bar{F} = A_3 - g\beta\bar{H} - g\beta'\bar{I} \tag{24}$$

$$\frac{d^2\bar{H}}{d\bar{y}^2} + A_6^2\bar{H} = 0 \tag{25}$$

$$G = A_1(cons\tan t) \tag{26}$$

$$\frac{d^2\bar{I}}{d\bar{y}^2} - A_9^2\bar{I} = 0 \tag{27}$$

Equation (24) to (27) are solved with boundary conditions in equation (23), the obtained solutions are:

$$\bar{H} = \left(\frac{\cos A_6\bar{y}}{2\cos A_6}\right) - \frac{\sin A_6\bar{y}}{2\sin A_6} \tag{28}$$

$$\bar{I} = \frac{\cosh A_9\bar{y}}{2\cosh A_9} - \frac{\sinh A_9\bar{y}}{2\sinh A_9} \tag{29}$$

$$F = \left\{\begin{aligned} &A_7 + A\cosh A_2 y + B\ \sinh A_2 y +\\ &A_8\cos A_6 y + A_9\sin A_6 y +\\ &A_{10}\cosh \Lambda y + A_{11}\sinh \Lambda y\end{aligned}\right\} \tag{30}$$

Blood velocity in the axial direction, using equation (30) with equation (19) is given by

$$\bar{u}(y,s) = \left(\begin{aligned} &A_7 + A\cosh A_2\bar{y} +\\ &B\ \sinh A_2\bar{y}\\ &+ A_8\cos A_6\bar{y} +\\ &A_9\sin A_6\bar{y} +\\ &+ A_{10}\cosh \Lambda 1\bar{y} +\\ &A_{11}\sinh \Lambda\bar{y}\end{aligned}\right)\frac{1}{s+\lambda^2} \tag{31}$$

Blood velocity in the normal direction to the bifurcated artery, using equation (26) with equation (21) is given by

$$\bar{v}(y,s) = A_1\frac{1}{s+\lambda^2} \tag{32}$$

Temperature distribution in the bifurcated arteries is given by equation (28) with (20):

$$\bar{\theta}(y,s) = \left(\left(\frac{\cos A_6\bar{y}}{2\cos A_6}\right) - \frac{\sin A_6\bar{y}}{2\sin A_6}\right)\frac{1}{s+\lambda^2} \tag{33}$$

The flowing blood in the carotid artery caries drug as concentration is given by equation (22) with (29):

$$\bar{C}(y,s) = \left(\frac{\cosh A_9\bar{y}}{2\cosh A_9} - \frac{\sinh A_9\bar{y}}{2\sinh A_9}\right)\frac{1}{s+\lambda^2} \tag{34}$$

Equations (31) to (34) are subjected to inverse Laplace transform, employing Gerby-Stephan's Algorithm. The obtained results are then visualized through graphical simulations using MATHCAD software, as presented and elaborated upon in the subsequent section.

5. Results and Discussion

We employed MATHCAD software to analysed flow data extracted from numerical results obtained via analytical solutions (31), (33), and (34). Graphical representations are provided for fractional parameters, velocity, temperature, and blood concentration. The impact of various dimensionless parameters, including magnetic field parameters (M), radiation number (R), fractional parameters (α), heat source parameters (S), Schmidt number (Sc), among others, on fluid velocity, temperature, and concentration were investigated. The magnetic field consistently showed a greater influence on the velocity profile, primarily due to its application increasing the resistive force, known as the Lorentz force, thereby constraining fluid flow within the system. Figure 2 illustrates this effect. Blood velocity significantly decreased with increasing values of the magnetic field parameter for fractional orders (α=0.4) while decreasing slowly for integer orders (α=1). Consequently, controlled magnetic fields hold promise for therapeutic applications and treatments related to conditions such as atherosclerosis, bone fractures, controlled tissue damage, and cancer [42].

Figure 3 demonstrates the change in blood velocity at different values of the heat source parameter (S) for both fractional and classical blood flow. Blood velocity is observed to increase as the heat source increases and is minimal for fractional fluids (α=0.4). However, axial velocity increases symmetrically with an increase in the heat source parameter.
Figure 4 illustrates the velocity distribution at different thermal radiation parameters (R). Blood velocity increases with increasing radiation parameter (R) for both fractional and classical orders, aligning with observations in Newtonian fluid models. Thermal radiation indirectly affects the velocity profile by influencing the effective viscosity of fluids.

Figure 5 shows the effect of applied magnetic field parameters for different tilt values. Increasing the angle of inclination of the applied magnetic field decreases blood flow for both fractionated and classical fluids across the affected area. Notably, flow velocity disappears between angles of 80° to 85° for fractionated fluids.

Figure 6 depicts the blood flow velocity profile at four different times (t=0.01 and 0.5) with five different values of fractional parameters α=0.2,0.4,0.6,0.8, and 1). The fractional parameter (α) plays a pivotal role in controlling blood velocity. At initial stages (t = 0.01), fluids with fractional derivatives exhibit faster flow velocities compared to integer order fluid models. However, an opposite trend is observed for longer periods (t = 0.5), where the velocity of integer order fluids surpasses that of fractional order fluids. This phenomenon is attributed to the system's stability, which tends to increase over longer time periods. Generally, blood velocity increases with increasing time for both fractional and integer order fluid models.

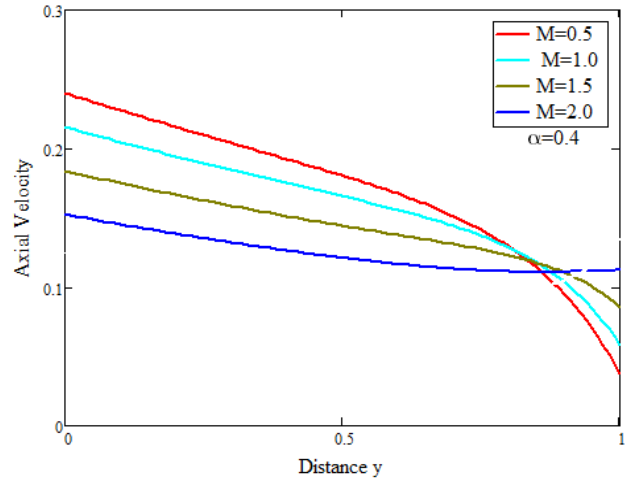

(2a)

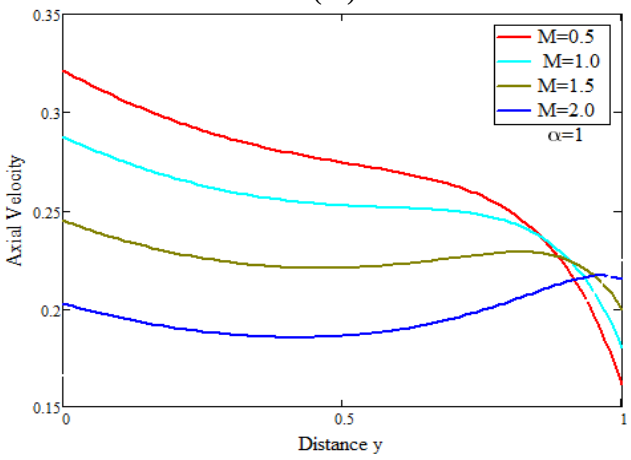

(2b)

Fig.2: Axial velocity profile for Different values of Magnetic Parameter (a) $\alpha = 0.4$ (b) $\alpha = 1$

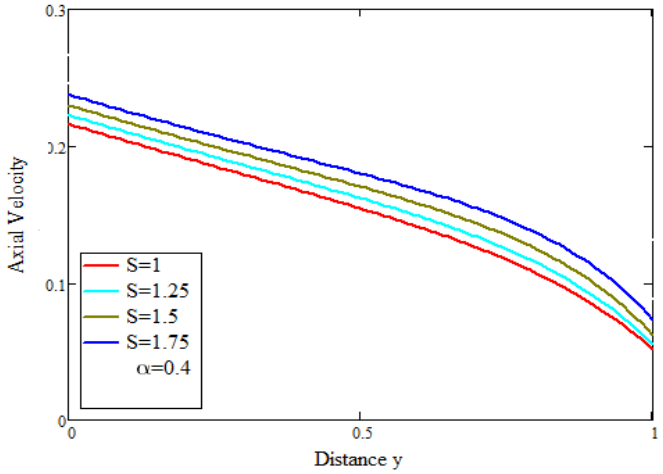

(3a)

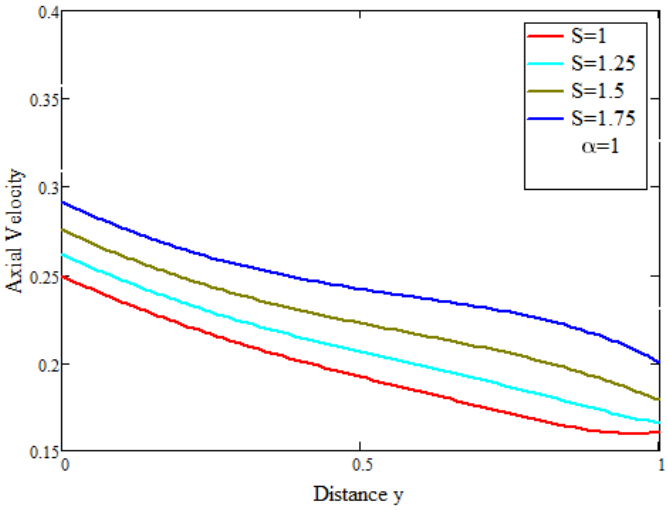

(3b)

Fig.3 Axial velocity profile for Different values of Heat Source Parameter (a) $\alpha = 0.4$ (b) $\alpha = 1$
$\omega = 0.5, M = 0.5, P_r = 2, K = 2,$
$R = 0.5, t = 1, h = 0.5, \beta = 0.5, \phi = 30^0, Sc = 0.5,$

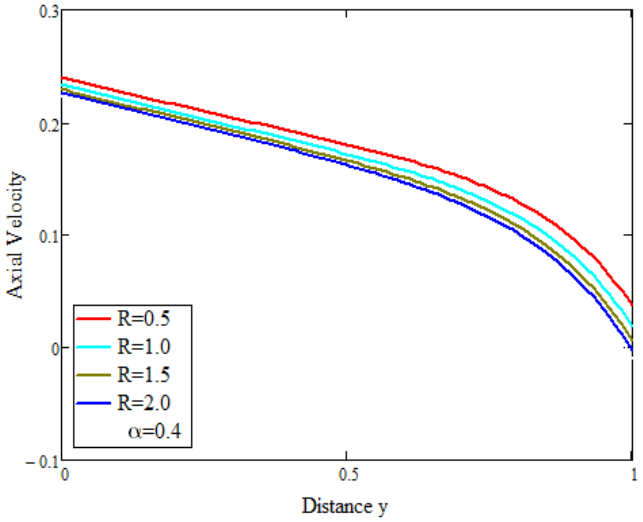

(4a)

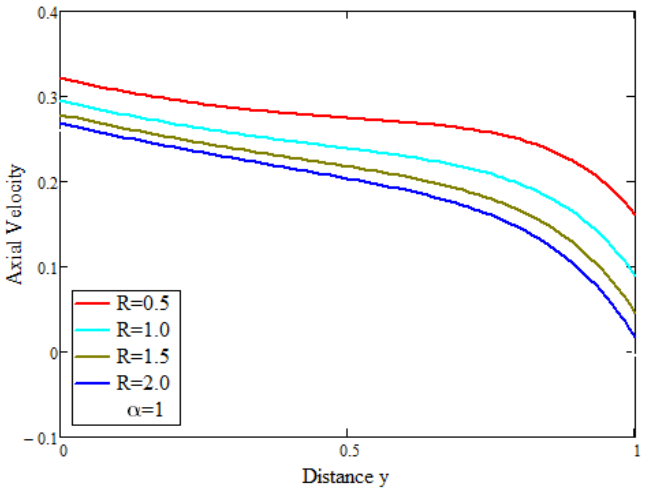

(4b)

Fig.4: Axial velocity profile for Different values of Radiation Parameter (a) $\alpha = 0.4$ (b) $\alpha = 1$

$\omega = 0.5, S = 1, P_r = 2, K = 2, M = 0.5,$

$t = 1, h = 0.5, \beta = 0.5, \phi = 30^0, Sc = 0.5,$

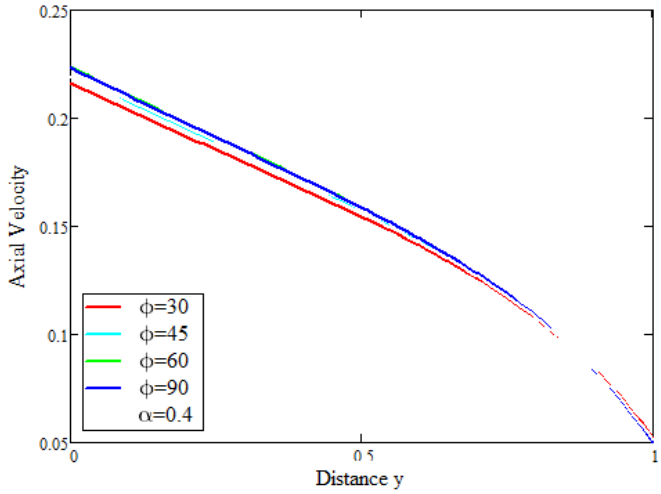

(5a)

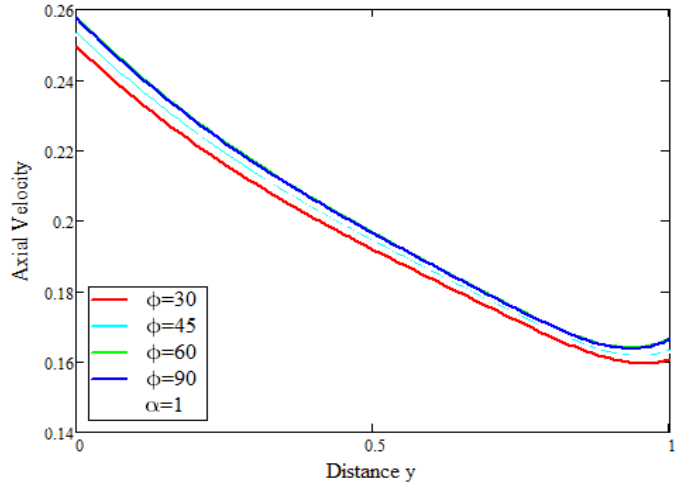

(5b)

Fig.5 Axial velocity profile for Different values of Angles of Inclination of Magnetic Field

(a) $\alpha = 0.4$ (b) $\alpha = 1$

$\omega = 0.5, S = 1, P_r = 2, K = 2, M = 0.5,$

$t = 1, h = 0.5, \beta = 0.5, \phi = 30^0, Sc = 0.5,$

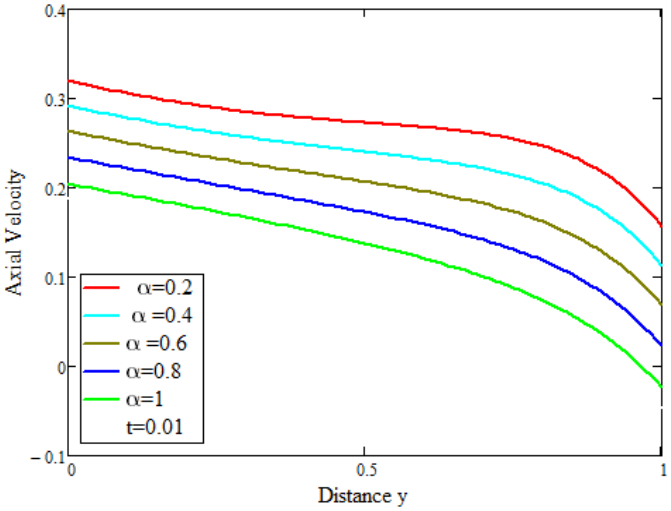

(6a)

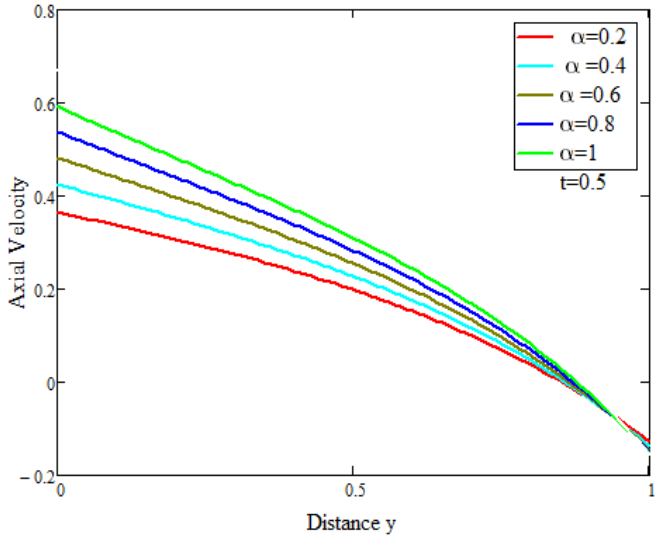

(6b)

Fig.6 Axial velocity profile for Different values α at (a) $t = 0.01$ (b) $t = 0.5$

$\omega = 0.5, S = 1, P_r = 2, K = 2, M = 0.5,$

$t = 1, h = 0.5, \beta = 0.5, \phi = 30^0, Sc = 0.5,$

Figures (7) to (9) depict temperature profiles for various values of the radiation parameter (R), fractional parameter (α), and heat source parameter (S). Figure 7 showcases the temperature variation for different radiation parameters (R). It is clear that temperature magnitude increases with higher levels of thermal radiation for both fractional and integer order derivatives. Particularly, temperatures are elevated along the centre line for integer order derivatives, a distribution pattern crucial for hyperthermia. Hyperthermia, characterized by the body's inability to regulate temperature, occurs when the body absorbs heat from external sources or experiences temperature dysregulation. In hyperthermia,

blood internal temperature rises without affecting the surrounding tissue of the blood vessel. Therefore, in our model, we neglect temperature exchange at the artery wall, setting the wall temperature to zero. Consequently, in the present model, blood temperature is minimal at the arterial wall and higher at the midline for classical fluids. This phenomenon aligns with findings from theoretical and experimental studies on non-Newtonian and Newtonian fluids of integer order. Another influential parameter similar to radiation is the heat source (S), significantly affecting temperature distribution within the bloodstream. Figure 8 demonstrates the thermal effects associated with heat production processes influenced by a higher number of mitochondria per cell, resulting in increased heat production within the system. It is observed that blood vessel temperature is lower in the absence of a heat source, while the addition of a heat source elevates temperature distribution within the blood flow system, maintaining a zero-wall temperature according to boundary conditions. The temperature distribution is notably affected by variations in the fractional parameter, as depicted in Figure 9. Here, it is evident that temperature increases with higher fractional parameter values, indicating that temperature distribution for fractional order fluid models is consistently higher across various instances.

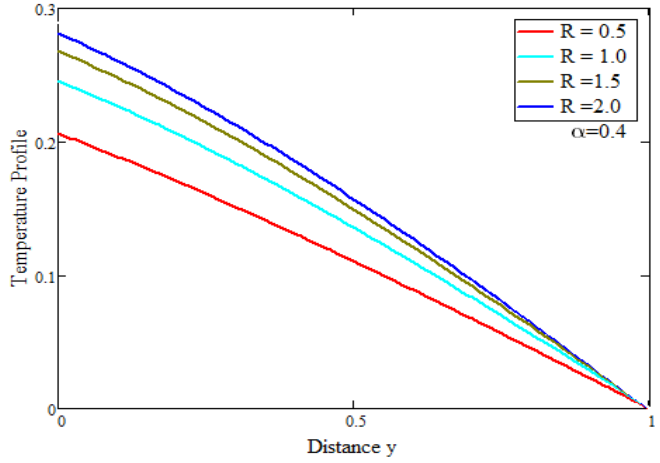

(7a)

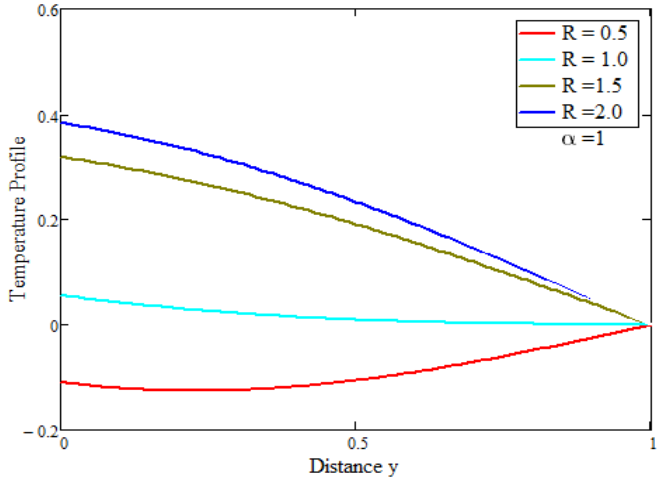

(7b)

Fig.7 Temperature profile for Different values of Radiation Parameter (a) $\alpha = 0.4$ (b) $\alpha = 1$

$\omega = 0.5, S = 1, P_r = 2, K = 2, M = 0.5,$

$t = 1, h = 0.5, \beta = 0.5, \phi = 30^0, Sc = 0.5,$

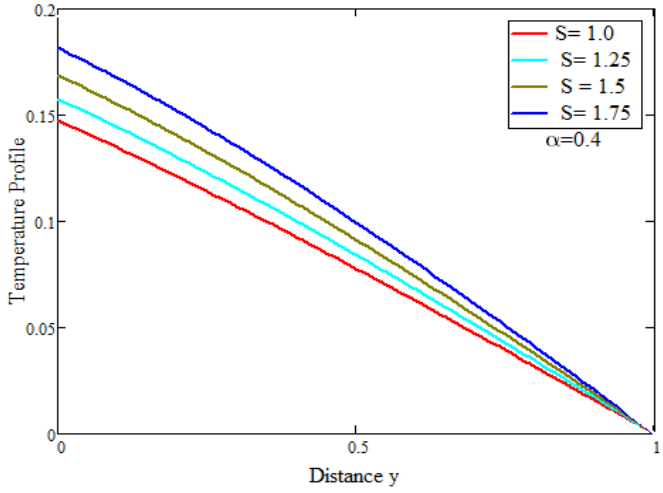

(8a)

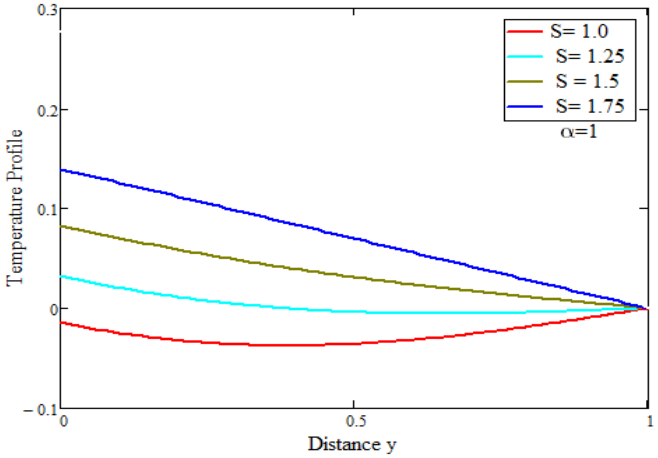

(8b)

Fig.8. Temperature profile for Different values of Heat Source Parameter (a) $\alpha = 0.4$ (b) $\alpha = 1$

$\omega = 0.5, R = 0.5, P_r = 2, K = 2, M = 0.5,$

$t = 1, h = 0.5, \beta = 0.5, \phi = 30^0, Sc = 0.5,$

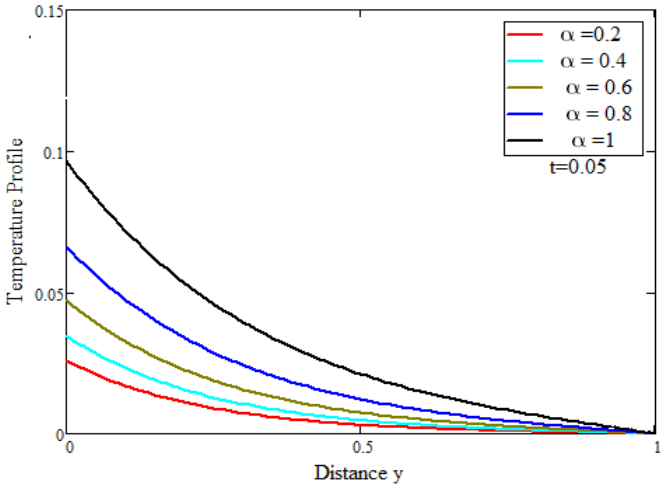

(9a)

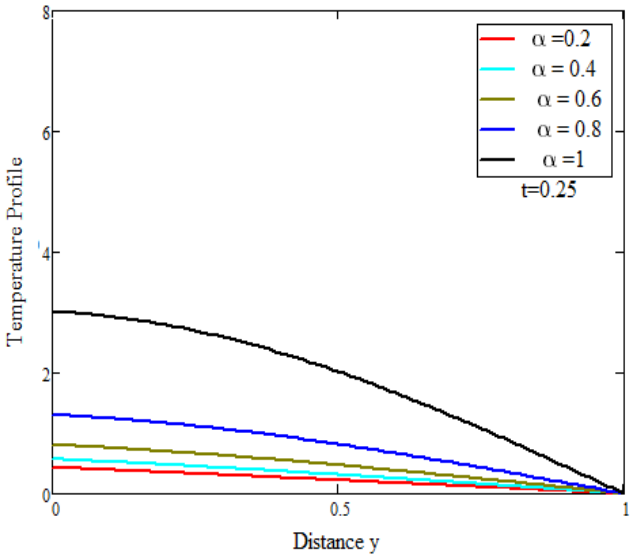

(9b)

Fig.9: Temperature profile for Different values of α at (a) $t = 0.05$ (b) $t = 0.25$

$$\omega = 0.5, S = 1, P_r = 2, K = 2, M = 0.5,$$
$$t = 1, h = 0.5, \beta = 0.5, \phi = 30^{o}, Sc = 0.5,$$

Figures 10 to 12 depict concentration profiles for varying Schmidt numbers, chemical reaction rates, and fractional parameters. Blood concentration denotes the density of blood cells suspended in plasma, with red blood cells (RBCs) being particularly influential due to their size and density. Due to their rotational behavior, RBCs tend to aggregate near the central area of the vessel, resulting in higher solute concentrations. In contrast, the off-axis region, primarily comprising plasma, exhibits minimal solute concentration. This concentration distribution pattern is consistently observed across all concentration plots. Importantly, the fractional model fluid demonstrates higher concentrations than the integer order fluid within shorter time intervals, as shown in Figure 10. This difference arises from the presence of fractional order derivatives in the model, which restrict fluid flow. Conversely, an opposite trend is noted for the Schmidt number. The inclusion of the Schmidt number introduces an additional force due to temperature gradients in blood cells, thereby augmenting concentration, as depicted in Figure 11. The concentration amplitude of blood flow is higher for integer order derivatives. Chemical reaction parameters for both fractional and integer derivatives notably reduce solute concentration, with this effect particularly prominent along the flow axis (x) and gradually diminishing in the (y) region for both fractional and integer order derivatives.

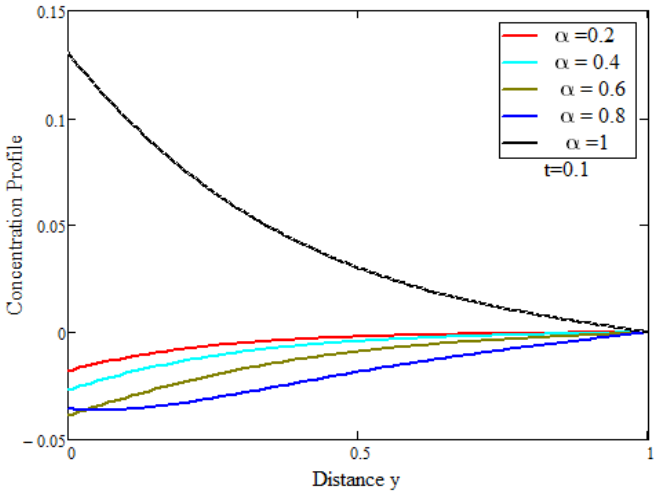

(10a)

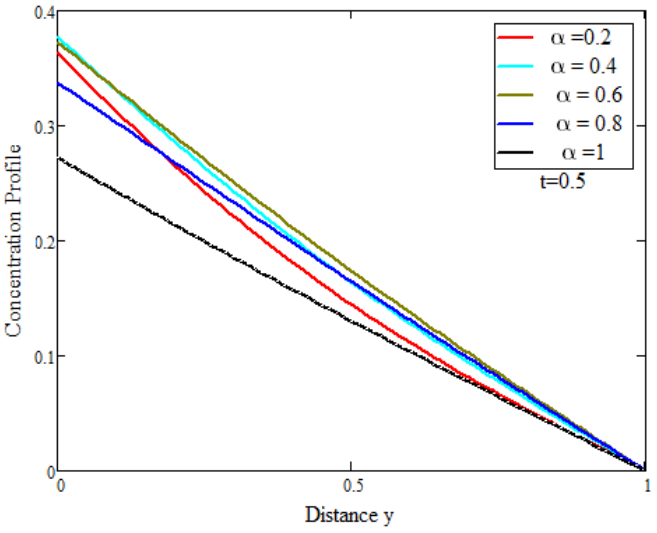

(10b)

Fig.10: Concentration profile for Different values of α at (a) $t = 0.1$ (b) $t = 0.5$

$$Sc = 0.5, S = 1, P_r = 2, K = 2, M = 0.5,$$
$$t = 1, h = 0.5, \beta = 0.5, \phi = 30^{o}, R = 0.5,$$

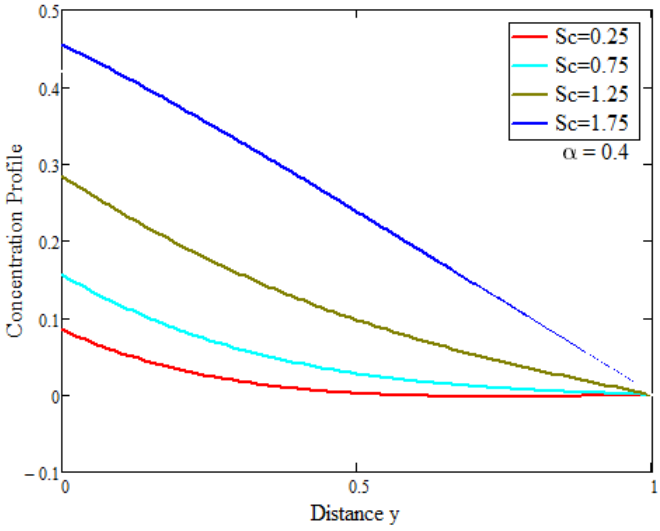

(11a)

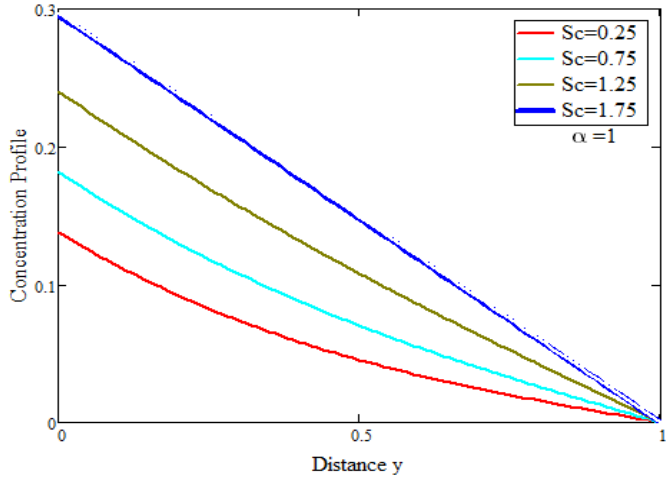

(11b)

Fig.11. Concentration profile for Different values of Schmidt Number (a) $\alpha = 0.4$ (b) $\alpha = 1$

$\omega = 0.5, S = 1, P_r = 2, K = 2, M = 0.5,$

$t = 1, h = 0.5, \beta = 0.5, \phi = 30^0, R = 0.5,$

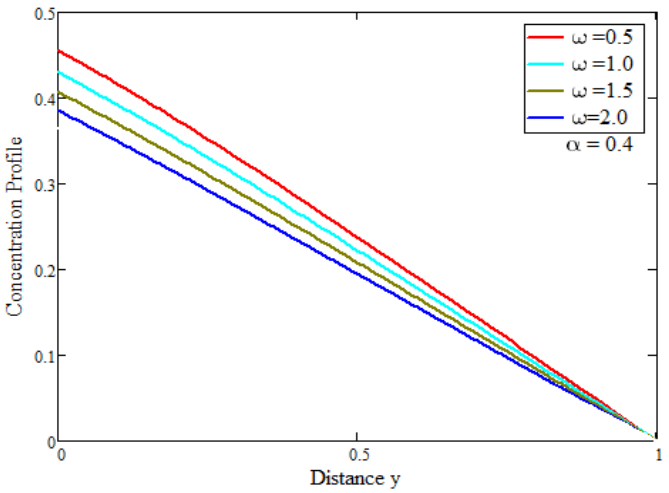

(12a)

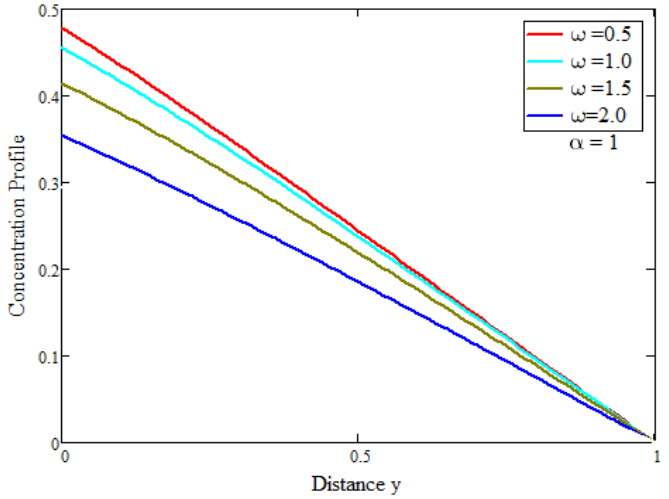

(12b)

Fig.12: Concentration profile for Different values of Schmidt Number (a) $\alpha = 0.4$ (b) $\alpha = 1$

$Sc = 0.5, S = 1, P_r = 2, K = 2, M = 0.5,$

$t = 1, h = 0.5, \beta = 0.5, \phi = 30^0, R = 0.5,$

6. Conclusion

The main objective of this mathematical analysis is to develop a fractional-order model that describes magnetohydrodynamic blood flow through bifurcated arteries in the presence of an inclined magnetic field, thermal radiation, and heat source, particularly focusing on applications in tumor treatments. The solution to this mathematical model is achieved through a combination of Laplace transform and the undetermined coefficient method, utilizing the specified constraint transformations. Notably, the distributions of velocity, temperature, and concentration are significantly influenced by the fractional order parameter. Initially, the flow modelled with fractional order exhibits higher velocities compared to integer order fluid flow. However, as dimensionless time progresses, fractional fluid flow slows down relative to integer-order fluid flow. The impact of fluid velocity is particularly noticeable in the slower rate of increase in fluid velocity with higher values of the magnetic field parameter. Furthermore, blood flow concentration decreases with increasing chemical reaction parameters, while an increase in the Schmidt number results in higher blood concentration. The dimensionless temperature of blood flow rises with increasing values of the fractional parameter and the heat source, which also affects the radiation parameter similarly. Understanding and analyzing these results are crucial in the context of hyperthermia treatment for cancer therapy, and they may offer insights into concentration phenomena of drug particles for drug delivery applications.

Availability of Data and Materials:
Not applicable

Conflict of Interest:
The authors declare that there are no conflicts of interest related to the study. This is an important declaration to ensure transparency and to address any potential biases that could arise from financial or personal relationships.

Funding:
The study received no external support.

Authors' Contributions Statement:
All authors contributed equally to the work and approved the final version of the manuscript.

Acknowledgment:
The authors gratefully acknowledged the reviewers and the Editor in-chief for their comments and necessary suggestions.

Appendix

$$A_1 = 1, A_2 = M^2 \sin^2 \phi - \frac{1}{k} - \frac{s}{(1-\alpha)s+\alpha},$$

$$A_3 = h(s+\lambda^2), A_4 = \frac{\tau p_r}{R\tau p_r + 1}$$

$$A_5 = \left(\frac{S}{\tau p_r} - \frac{S}{(1-\alpha)s+\alpha} \right)(s+\lambda^2),$$

$$A_6 = \sqrt{A_4 A_5}, \quad A_7 = \frac{A_3}{A}$$

$$A_9 = \sqrt{Sc(\omega + s((1-\alpha)s+\alpha)},$$

$$A_{10} = \frac{-g\beta}{2(A_9^2 - A_2)\cosh A_9},$$

$$A_{11} = \frac{g\beta}{2(A_9^2 - A_2)\sinh A_9}$$

References

[1] E. E. Tzirtzilakis, "A mathematical model for blood flow in magnetic field," Phys. Fluids, vol. **17**, pp**. 077103-1–077103-15, 2005**.

[2] J. C. Chato, "Heat transfer to blood vessels," J. Biomech. Eng., vol. **102**, no. **2**, pp. **110–118, 1980.**

[3] S. Shaw and P. V. S. N. Murthy, "Magnetic drug targeting in the permeable blood vessel—The effect of blood rheology," J. Nanotechnol. Eng. Med., vol. **1**, no. **2**, pp. **021001-1–021001-11, 2010.**

[4] G. C. Shit and S. Majee, "Pulsatile flow of blood and heat transfer with variable viscosity under magnetic and vibration environment," J. Magn. Magn. Mater., vol. **388**, pp. **106–115, 2015**.

[5] J. C. Misra and G. C. Shit, "Flow of a biomagnetic visco-elastic fluid in a channel with stretching walls," J. Appl. Mech., vol. **76**, no. 6, pp. **061006-1–061006-6, 2009.**

[6] A. Mondal and G. C. Shit, "Transport of magneto-nanoparticles during electro-osmotic flow in a micro-tube in the presence of a magnetic field for drug delivery application," J. Magn. Magn. Mater., vol. **442**, pp. **319–328, 2017.**

[7] M. M. Bhatti, A. Zeeshan, and R. Ellahi, "Simultaneous effects of coagulation and variable magnetic field on peristaltically induced motion of Jeffrey nanofluid containing gyrotactic microorganism," Microvasc. Res., vol. 110, pp. **32–42, 2017**.

[8] M. Abdulhameed, D. Vieru, and R. Roslan, "Modeling electro-magnetohydrodynamic thermo-fluidic transport of biofluids with new trend of fractional derivative without singular kernel," Physica A, vol. **484**, pp. **233–252, 2017**.

[9] M. M. Bhatti, A. Zeeshan, R. Ellahi, "Endoscope analysis on peristaltic blood flow of Sisko-fluid with titanium magneto-nanoparticles," Comput. Biol. Med., vol. **78,** pp. **29–41, 2016.**

[10] A. Zeeshan, M. M. Bhatti, N. S. Akbar, and Y. Sajjad, "Hydromagnetic blood flow of Sisko-fluid in a non-uniform channel induced by peristaltic wave," Commun. Theor. Phys., vol**. 68**, pp. **103–110, 2017.**

[11] S. Majee and G. C. Shit, "Numerical investigation of MHD flow of blood and heat transfer in a stenosed arterial segment," J. Magn. Magn. Mater., vol. **424**, pp. **137–147, 2017**.

[12] N. S. Akbar and A. W. Butt, "Entropy generation analysis in convective ferromagnetic nano blood flow through a composite stenosed arteries with permeable wall," Commun. Theor. Phys., vol. **67,** pp**. 554–560, 2017.**

[13] S. G. Samko, A. A. Kilbas, and O. I. Marichev, "Fractional integrals and derivatives: Theory and applications," Gordon and Breach Science Publishers, **1993**.

[14] S. Das, "Functional fractional calculus for system identification and controls," Springer, **2008.**

[15] K. Oldham and J. Spanier, "The fractional calculus," Academic Press, **1974**.

[16] M. D. Ortigueira, "Fractional Calculus for Scientists and Engineers," Springer, New York, **2011.**

[17] D. Baleanu, K. Diethelm, E. Scalas, and J. J. Trujillo, "Fractional calculus models and numerical methods," World Scientific Publishing Company, Singapore, **2012**.

[18] D. A. MacDonald, "On steady flow through modeled vascular stenosis," J. Biomech., vol. 12, no. **1,** pp**. 13–20, 1979**.

[19] C. G. Caro, T. J. Pedley, R. C. Schroter, and W. A. Seed, "The Mechanics of the Circulation," Cambridge University Press, **2012.**

[20] D. Liepsch, "Flow in tubes and arteries- A Comparison," Biorheology, vol. **23,** pp. **395–433, 1986.**

[21] L. Srivastava and V. Srivastava, "Peristaltic transport of blood: Casson model-II," J. Biomech., vol. **17,** no**. 11,** pp**. 821–829, 1984**.

[22] P. Nagarani, G. Sarojamma, and G. Jayaraman, "Exact analysis of unsteady convective diffusion in Casson fluid flow in an annulus-Application to catheterized artery," Acta Mechanica, vol. **187,** pp. **189–202, 2006.**

[23] J. Venkatesan, D. Sankar, K. Hemalatha, and Y. Yatim, "Mathematical analysis of Casson fluid model for blood rheology in stenosed narrow arteries," J. Appl. Math., vol. **2013,** pp. **1–11, 2013.**

[24] T. Hayat, S. Asad, and A. Alsaedi, "Flow of Casson fluid with nanoparticles," Appl. Math. Mech., vol. **37,** no**. 4,** pp. **479–490, 2016**.

[25] F. Ali, N. A. Sheikh, I. Khan, and M. Saqib, "Magnetic field effect on blood flow of Casson fluid in axisymmetric cylindrical tube: A fractional model," J. Magn. Magn. Mater., vol. **423,** pp**. 327–336, 2017**.

[26] M. Saqib, I. Khan, and S. Shafie, "Generalized magnetic blood flow in a cylindrical tube with magnetite dusty particles," J. Magn. Magn. Mater., vol. **484,** pp. **490–496, 2019**.

[27] V. F. Morales-Delgado, J. F. Gómez-Aguilar, K. M. Saad, M. A. Khan, and P. Agarwal, "Analytic solution for oxygen diffusion from capillary to tissues involving external force effects: A fractional calculus approach," Physica A, vol. **523,** pp. **4865, 2019**.

[28] S. He, N. A. A. Fataf, S. Banerjee, and K. Sun, "Complexity in the muscular blood vessel model with variable fractional derivative and external disturbances," Physica A, vol. **526,** pp. **120904, 2019.**

[29] Sunil, D. Sharma, and R. C. Sharma, "Effect of dust particles on thermal convection in ferromagnetic fluid saturating a porous medium," J. Magn. Magn. Mater., vol. **288,** pp**. 183–195, 2005.**

[30] K. Ramesh and M. Devakar, "Magnetohydrodynamic peristaltic transport of couple stress fluid through porous medium in an inclined asymmetric channel with heat transfer," J. Magn. Magn. Mater., vol. **394,** pp. **335–348, 2015.**

[31] G. C. Shit and M. Roy, "Pulsatile flow and heat transfer of a magnetomicropolar fluid through a stenosed artery under the influence of body acceleration," Int. J. App. Compt. Math., **vol. 1,** pp. **121–141, 2015**.

[32] M. M. Bhatti, A. Zeeshan, R. Ellahi, O. A. Beg, and A. Kadir, "Effects of coagulation on the two-phase peristaltic pumping of magnetized prandtl biofluid through an endoscopic annular geometry containing a porous medium," Chin. J. Phys., vol. **58,** pp**. 222–234, 2019**.

[33] R. K. Dash, K. N. Mehta, and G. Jayaraman, "Casson fluid flow in a pipe filled with homogeneous porous medium," Int. J. Engg. Sci., vol. **34**, pp. **1146–1156, 1996**.

[34] R. Bhargava, S. Rawat, H. S. Takhar, and O. A. Beg, "Pulsatile magnetobiofluid flow and mass transfer in a non-Darcian porous medium channels," Meccanica, vol. **42**, pp. **247–262, 2007.**

[35] S. E. Ghasemi, M. Hatami, A. K. Sarokolaie, and D. D. Ganji, "Study on blood flow containing nanoparticles through porous

arteries in presence of magnetic field using analytical methods," Physica E, vol. **70**, pp. **146–156, 2015**.

[36] M. M. Bhatti, A. Zeeshan, R. Ellahi, and G. C. Shit, "Mathematical modeling of heat and mass transfer effects on MHD peristaltic propulsion of two-phase flow through a Darcy-Brinkman-Forchheimer porous medium," Adv. Powder Tech., vol. **29**, pp. **1189–1197, 2018**.

[37] T. Chinyoka and O. D. Makinde, "Computational dynamics of arterial blood flow in the presence of magnetic field and thermal radiation therapy," Adv. Math. Phys., pp. **915640, 2014.**

[38] A. Sinha and G. C. Shit, "Electromagnetohydrodynamic flow of blood and heat transfer in a capillary with thermal radiation," J. Magn. Magn. Mater., vol**. 378**, pp. **143–151, 2015**.

[39] C. B. Tabi, T. G. Motsumi, C. D. B. Kamdem, and A. Mohamadou, "Nonlinear excitations of blood flow in large vessels under thermal radiations and uniform magnetic field," Commun. Nonl. Sci. Numer. Simul., vol. **49**, pp. **1–8, 2017.**

[40] S. Z. Alamri, A. A. Khan, M. Azeez, and R. Ellahi, "Effects of mass transfer on MHD second grade fluid towards stretching cylinder: A novel perspective of Cattaneo-Christov heat flux model," Phys. Lett. A, vol. **383,** pp. **276–281, 2019.**

[41] M. M. Bhatti, A. Zeeshan, and R. Ellahi, "Heat transfer analysis on peristaltically induced motion of particle-fluid suspension with variable viscosity: clot blood model," Comput. Math. Prog. Biomed., vol. **137**, pp. **115–124, 2016**.

[42] V. K. Sud and G. S. Sekhon, "Blood flow subject to a single cycle of body acceleration," Bull. Math. Biol., vol. **46,** pp**. 937–949, 1984**

